Electronic Supplementary Material (ESI) for Nanoscale.

Supporting Information

Oral supramolecular nanovectors for dual natural medicine codelivery to prevent gastric mucosal lesion

Supplementary Figure

Supplementary Table

Supplementary Table S1 Gastric lesion score standard.

Supplementary Methods and Results

Characteristics of E/C-SNs

Mucosal lesion assessment

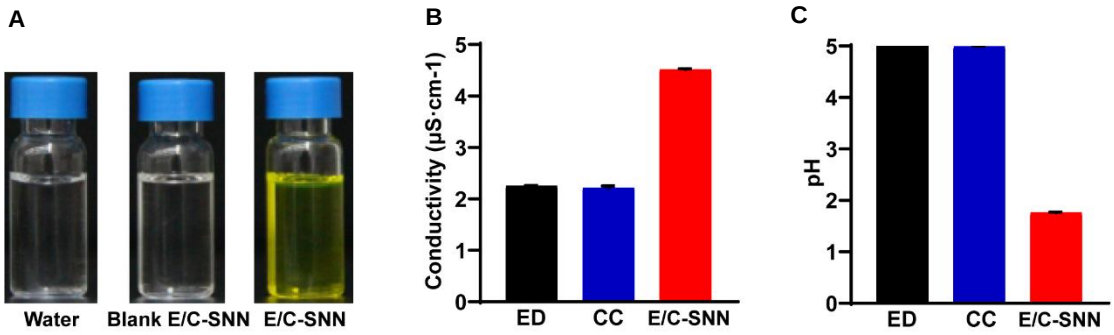

Supplementary Figure S1. Appearance, conductivity and pH values. (A) The appearance diagrams. (B) conductivity and (C) pH values of ED, CC and E/C-SNNs.

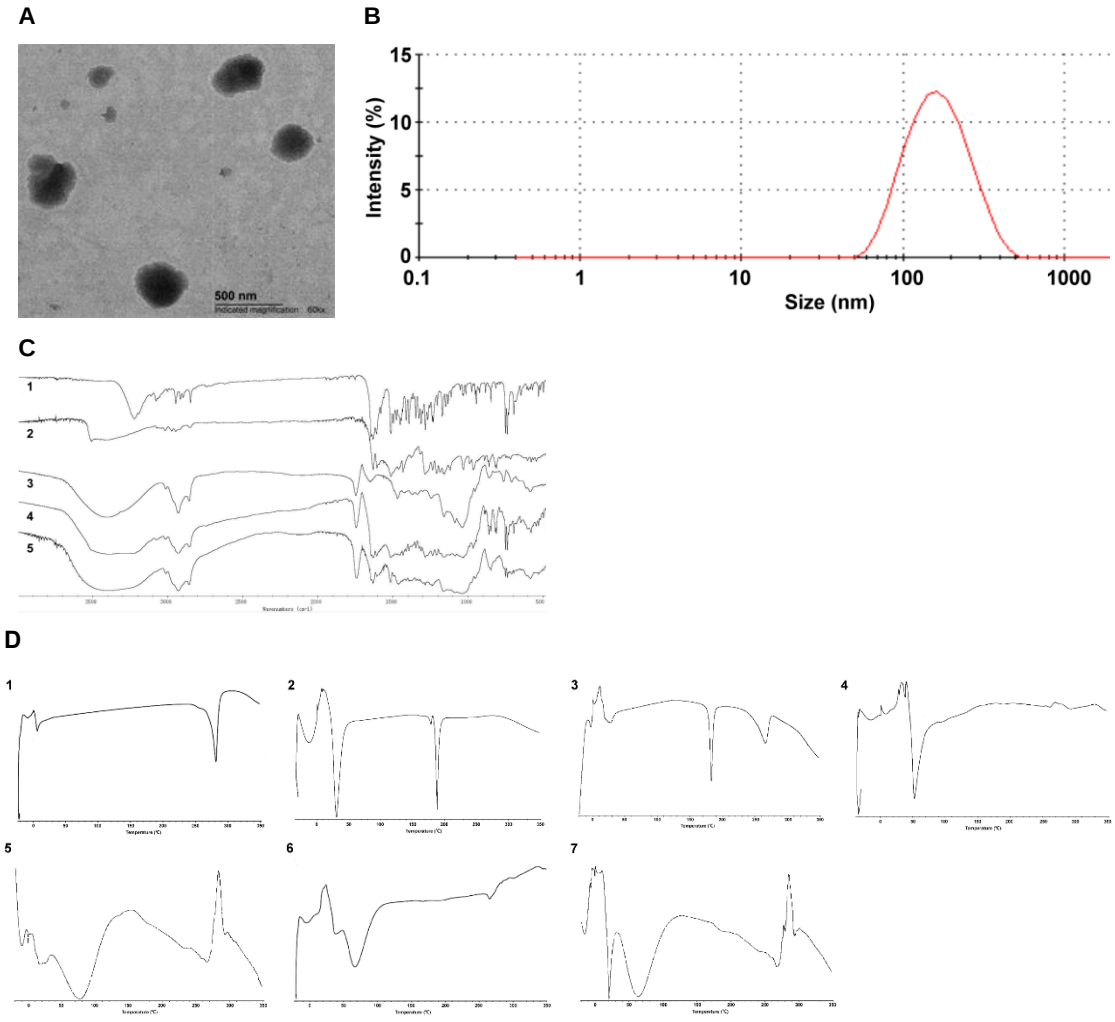

Supplementary Figure S2. Characterization of E/C-SN. (A) morphology measured by scanning electron microscopy (SEM). (B) particle size. (C) FT-IR. 1. ED, 2. CC, 3. physical mixture of PC and HPCD, 4. physical mixture of ED, CC, PC and HPCD, 5. E/C-SN. (D) DSC thermograms. 1. ED, 2. CC, 3. physical mixture of ED and CC, 4. physical mixture of PC and HPCD, 5. physical mixture of ED, CC, PC and HPCD, 6. Blank E/C-SN, 7. E/C-SN.

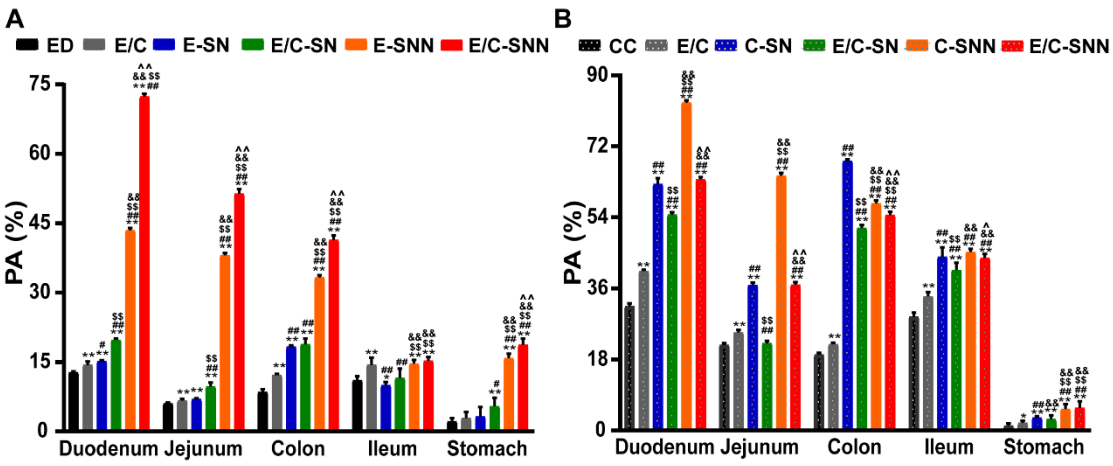

Supplementary Figure S3. Absorption percentage (PA) of (A) ED, E/C, E-SN, E/C-SN, E-SNN, E/C-SNN, (B) CC, E/C, C-SN, E/C-SN, C-SNN, E/C-SNN at gastrointestinal segments. Data are presented as the mean ± standard deviation (n = 6).*P<0.05 or **P<0.01 indicated significant difference or very significant difference compared to ED or CC; $^{\#}P$<0.05 or $^{\#\#}P$<0.01 indicated significant difference or very significant difference compared to E/C; $^{\$}P$<0.05 or $^{\$\$}P$<0.01 indicated significant difference or very significant difference compared to E-SN or C-SN; $^{\&}P$<0.05 or $^{\&\&}P$<0.01 indicated significant difference or very significant difference compared to E/C-SN; ^P<0.05 or ^^P<0.01 indicated significant difference or very significant difference compared to E-SNN or C-SNN group.

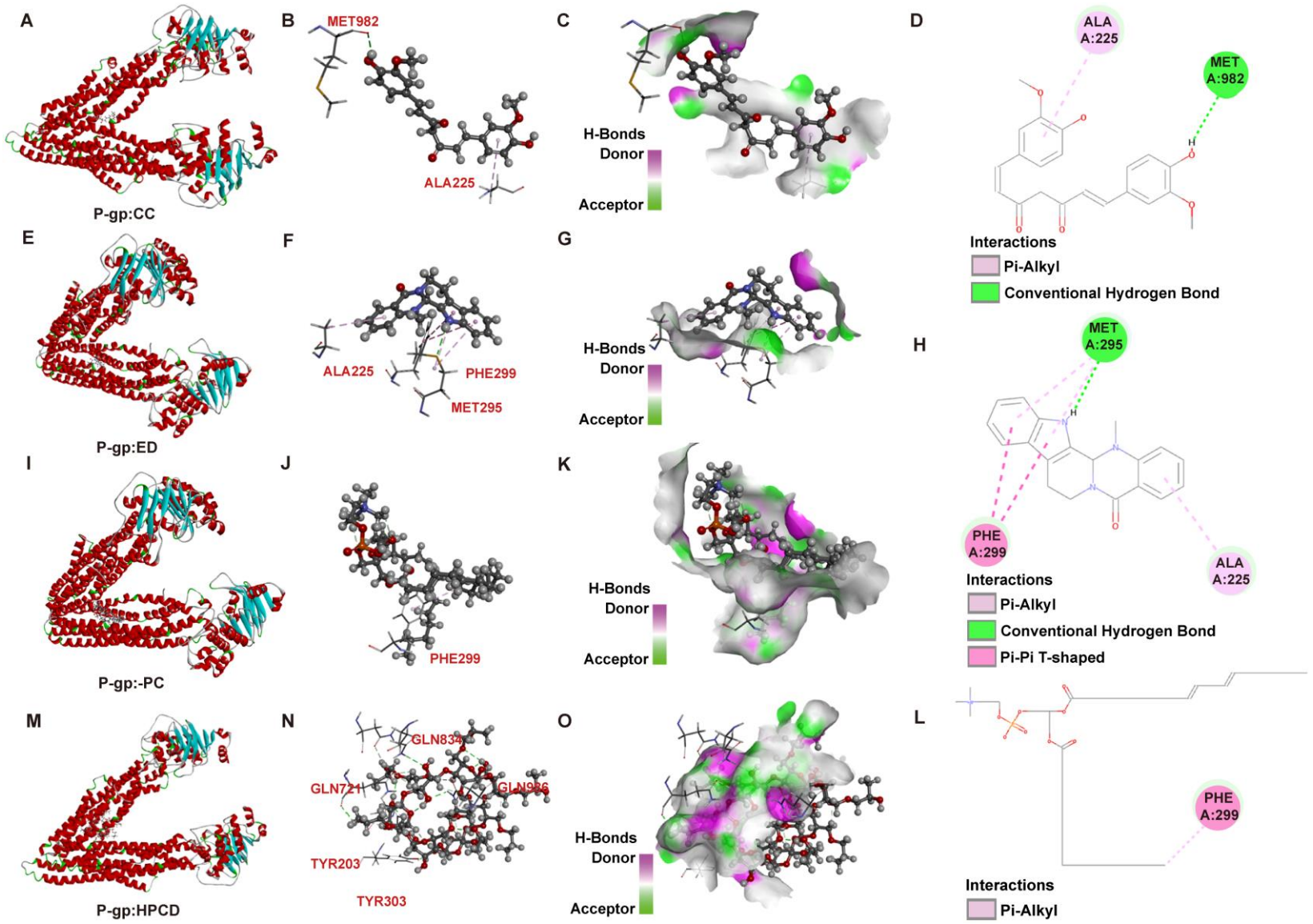
A
P-gp:CC
B
MET982
ALA225
C
H-Bonds
Donor
Acceptor
D
ALA
A:225
MET
A:982
Interactions
Pi-Alkyl
Conventional Hydrogen Bond
E
P-gp:ED
F
ALA225
PHE299
MET295
G
H-Bonds
Donor
Acceptor
H
MET
A:295
PHE
A:299
ALA
A:225
Interactions
Pi-Alkyl
Conventional Hydrogen Bond
Pi-Pi T-shaped
I
P-gp:-PC
J
PHE299
K
H-Bonds
Donor
Acceptor
L
PHE
A:299
Interactions
Pi-Alkyl
M
P-gp:HPCD
N
GLN834
GLN721
GLN986
TYR203
TYR303
O
H-Bonds
Donor
Acceptor

Supplementary Figure S4. Different views of the most probable complexes of P-glycoprotein (P-gp, 4XWK) and (A-D) ED, (E-H) CC, (I-L) PC and (M-O) HPCD. Ball and stick models are ED, CC, PC or HPCD.

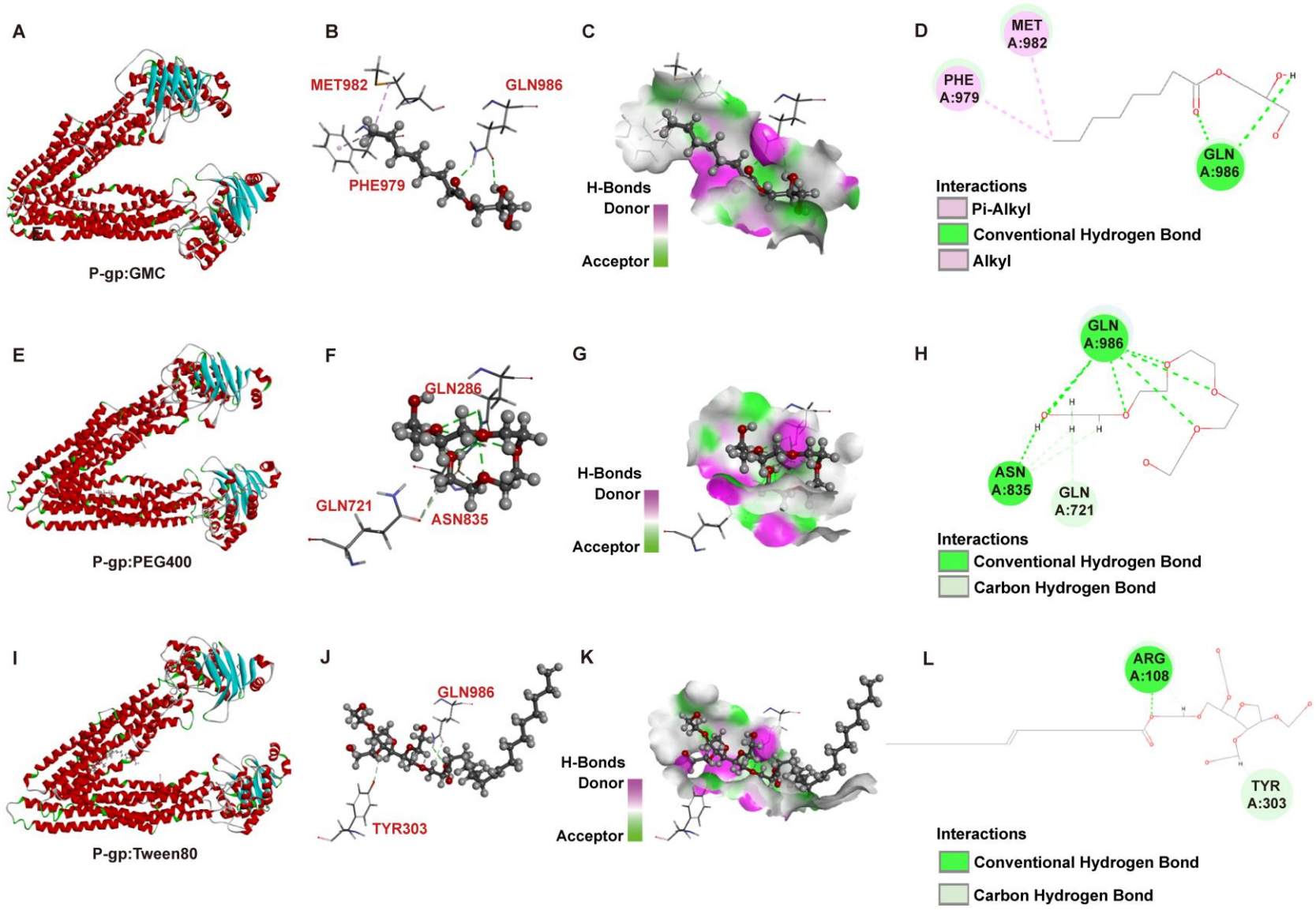
A
P-gp:GMC
B
MET982
GLN986
PHE979
C
H-Bonds
Donor
Acceptor
D
MET
A:982
PHE
A:979
GLN
A:986
Interactions
Pi-Alkyl
Conventional Hydrogen Bond
Alkyl
E
P-gp:PEG400
F
GLN286
GLN721
ASN835
G
H-Bonds
Donor
Acceptor
H
GLN
A:986
ASN
A:835
GLN
A:721
Interactions
Conventional Hydrogen Bond
Carbon Hydrogen Bond
I
P-gp:Tween80
J
GLN986
TYR303
K
H-Bonds
Donor
Acceptor
L
ARG
A:108
TYR
A:303
Interactions
Conventional Hydrogen Bond
Carbon Hydrogen Bond

Supplementary Figure S5. Different views of the most probable complexes of P-glycoprotein (P-gp, 4XWK) and (A-D) GMC, (E-H) PEG400 and (I-L) Tween80. Ball and stick models are GMC, PEG400, or Tween80.

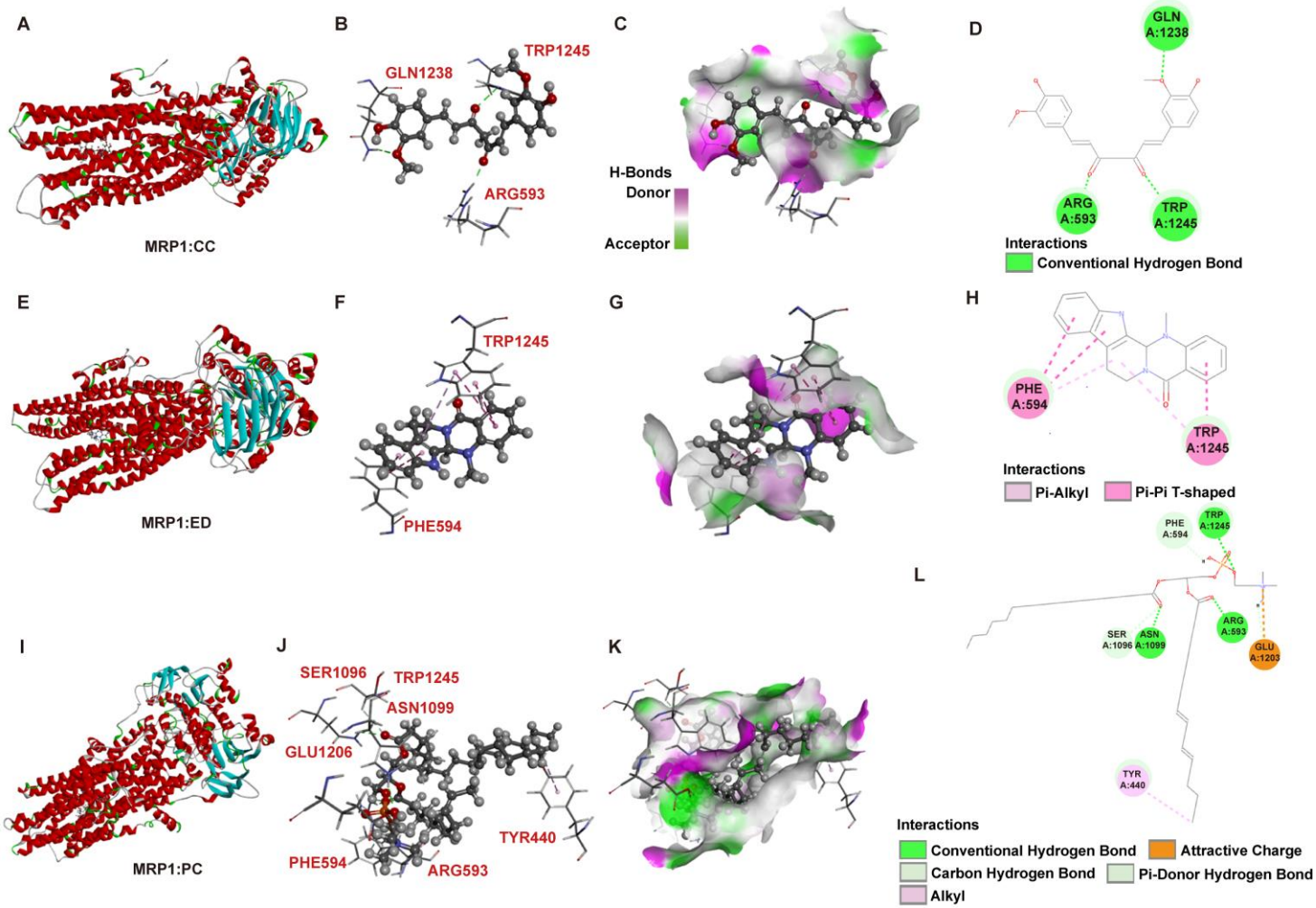
A
MRP1:CC
B
GLN1238
TRP1245
ARG593
C
H-Bonds
Donor
Acceptor
D
GLN A:1238
ARG A:593
TRP A:1245
Interactions
Conventional Hydrogen Bond
E
MRP1:ED
F
TRP1245
PHE594
G
H
PHE A:594
TRP A:1245
Interactions
Pi-Alkyl
Pi-Pi T-shaped
I
MRP1:PC
J
SER1096
TRP1245
ASN1099
GLU1206
TYR440
PHE594
ARG593
K
L
PHE A:594
TRP A:1245
SER A:1096
ASN A:1099
ARG A:593
GLU A:1203
TYR A:440
Interactions
Conventional Hydrogen Bond
Attractive Charge
Carbon Hydrogen Bond
Pi-Donor Hydrogen Bond
Alkyl

Supplementary Figure S6. Different views of the most probable complexes of multidrug resistance protein 1 (MRP1, PDB ID: 6UY0) and (A-D) ED, (E-H) CC and (I-L) PC. Ball and stick models are ED, CC, or PC.

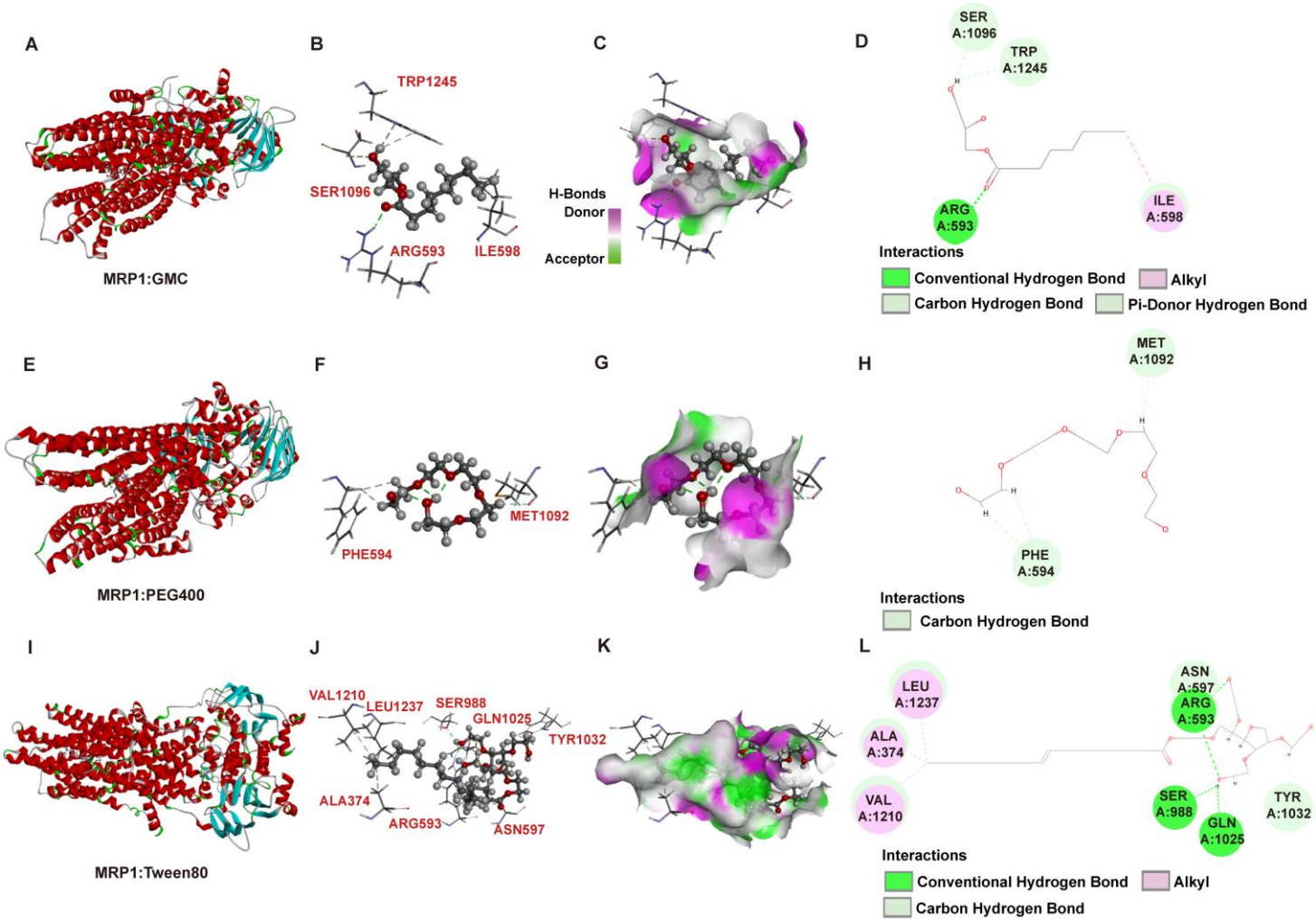
A
B
C
D
TRP1245
SER1096
ARG593
ILE598
H-Bonds
Donor
Acceptor
SER
A:1096
TRP
A:1245
ARG
A:593
ILE
A:598
Interactions
Conventional Hydrogen Bond
Alkyl
Carbon Hydrogen Bond
Pi-Donor Hydrogen Bond
MRP1:GMC
E
F
G
H
MET1092
PHE594
MET
A:1092
PHE
A:594
Interactions
Carbon Hydrogen Bond
MRP1:PEG400
I
J
K
L
VAL1210
LEU1237
SER988
GLN1025
TYR1032
ALA374
ARG593
ASN597
LEU
A:1237
ALA
A:374
VAL
A:1210
ASN
A:597
ARG
A:593
SER
A:988
GLN
A:1025
TYR
A:1032
Interactions
Conventional Hydrogen Bond
Alkyl
Carbon Hydrogen Bond
MRP1:Tween80

Supplementary Figure S7. Different views of the most probable complexes of multidrug resistance protein 1 (MRP1, PDB ID:6UY0) and (A-D) GMC, (E-H) PEG400 and (I-L) Tween80. Ball and stick models are GMC, PEG400, or Tween80.

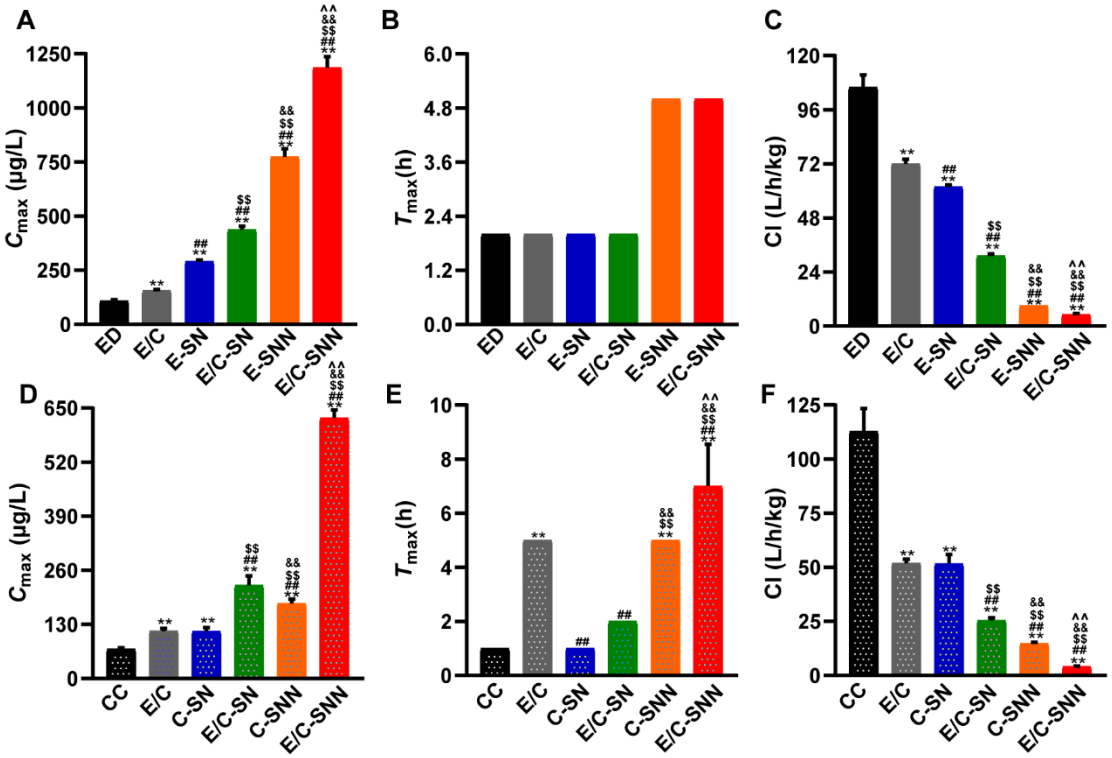

Supplementary Figure S8. Pharmacokinetic parameters of E/C-SNN. (A) C_{max}, (B) T_{max}, (C) *Cl* values of ED, E/C, E-SN, E/C-SN, E-SNN, E/C-SNN, when calculated as ED. (D) C_{max}, (E) T_{max}, (F) *Cl* values of ED, E/C, E-SN, E/C-SN, E-SNN, E/C-SNN, when calculated as CC.

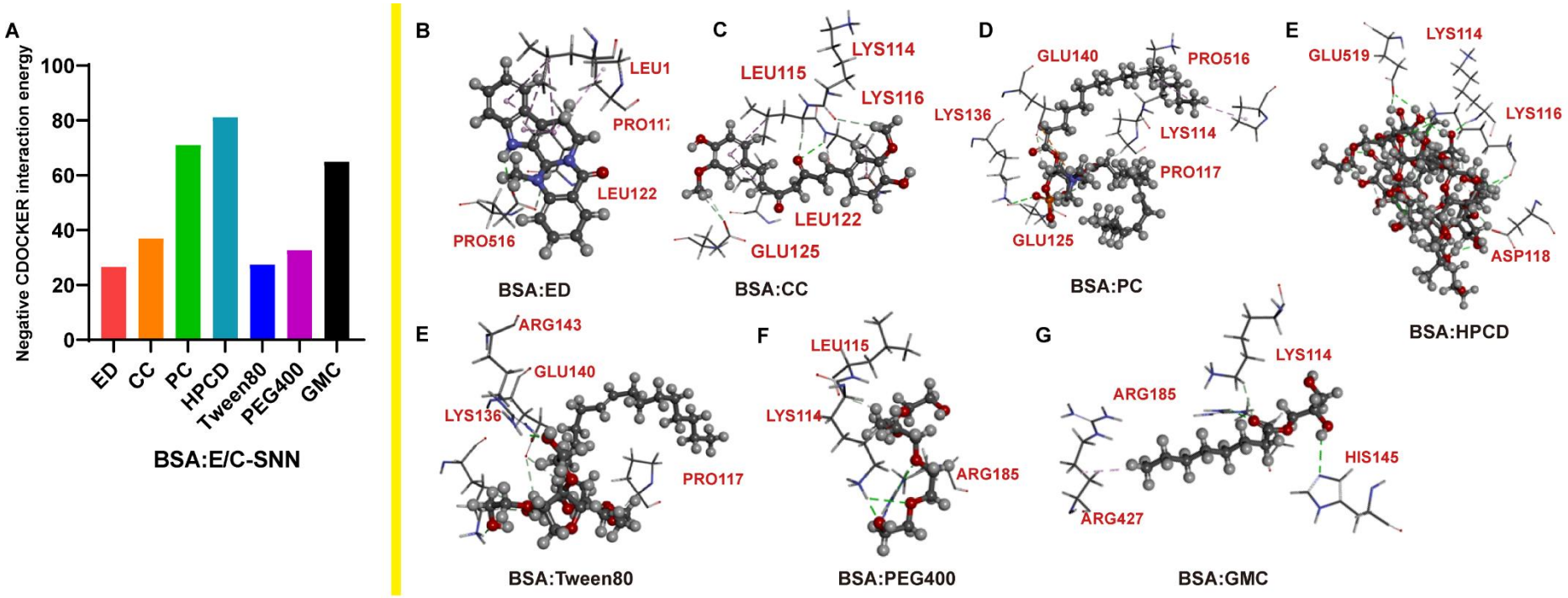

Supplementary Figure S9. Possible complexes of bovine serum albumin (BSA) and dual drug or E/C-SNN component. (A) negative CDOCER interaction energy values of BSA and ED, CC or E/C-SNN components. (B-G) electrical interactions of residues of BSA with (B) ED, (C) CC, (D) PC, (E) HPCD, (F) Tween 80, (G) PEG400. (H) GMC.

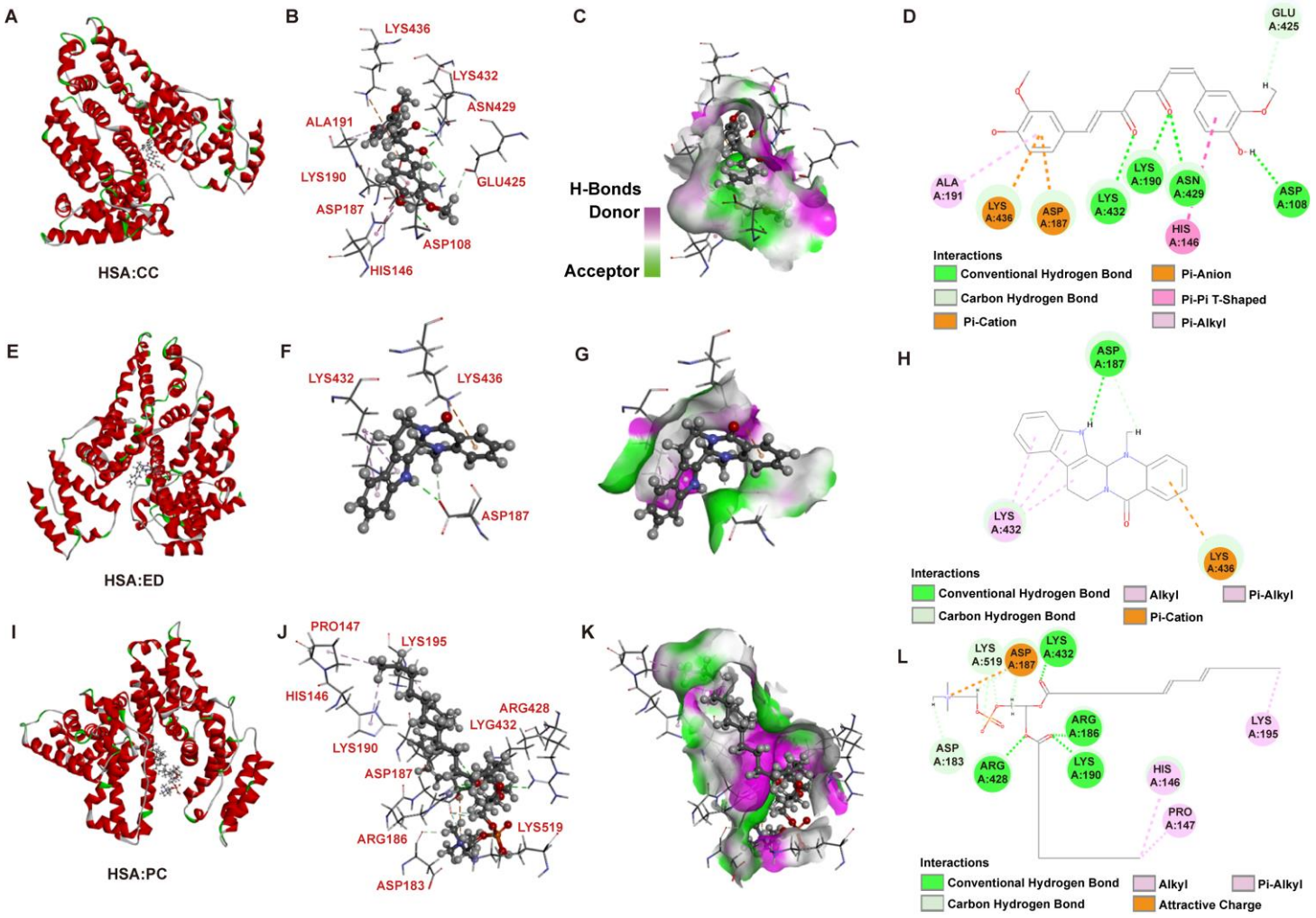

Supplementary Figure S10. Different views of the most probable complexes of human serum albumin (HAS, PDB ID: 1AO6) and (A-D) ED, (E-H) CC and (I-L) PC. Ball and stick models are ED, CC or PC.

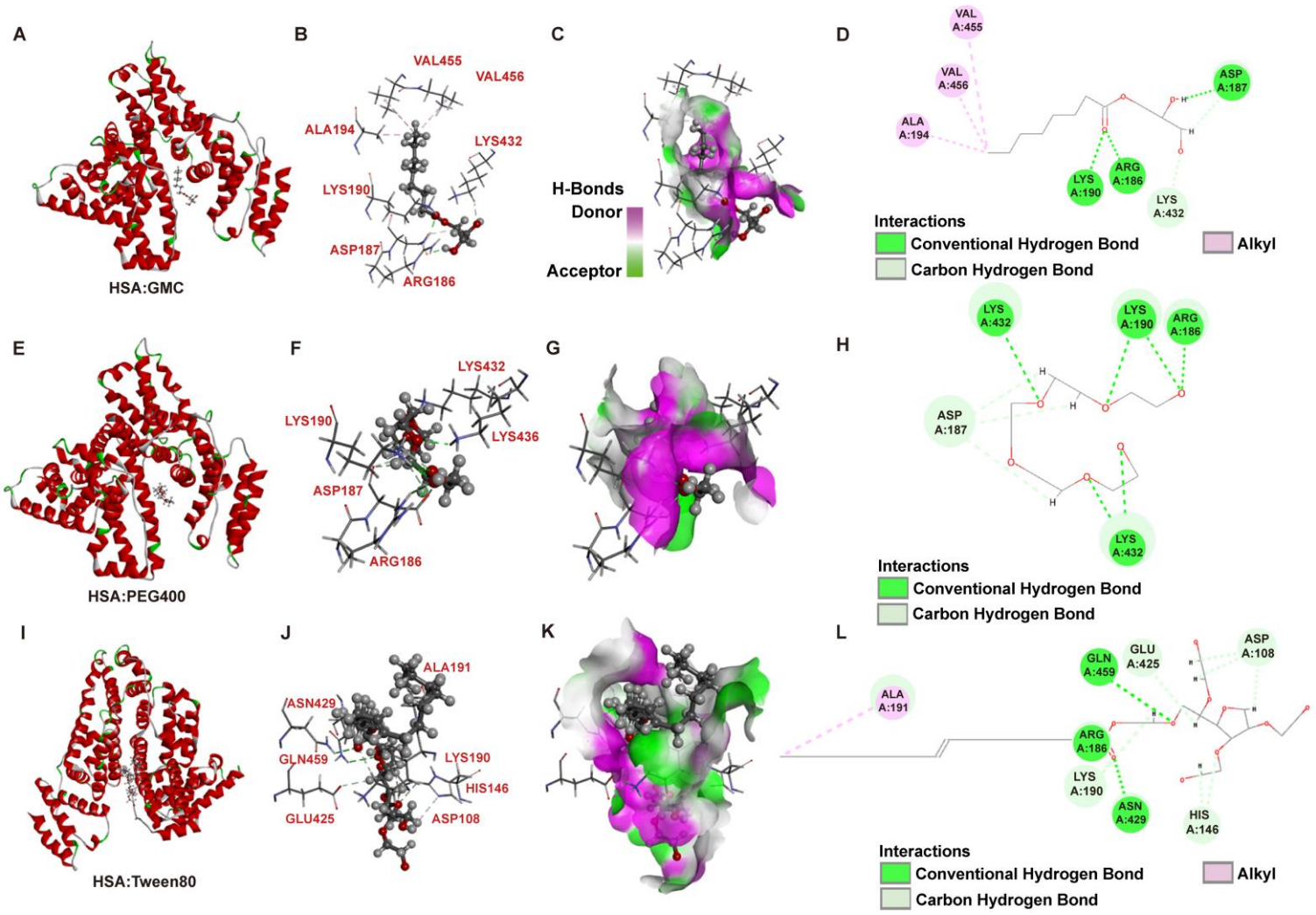
A
HSA:GMC
B
VAL455
VAL456
ALA194
LYS432
LYS190
ASP187
ARG186
C
H-Bonds
Donor
Acceptor
D
VAL A:455
VAL A:456
ALA A:194
ASP A:187
LYS A:190
ARG A:186
LYS A:432
Interactions
Conventional Hydrogen Bond
Carbon Hydrogen Bond
Alkyl
E
HSA:PEG400
F
LYS432
LYS190
LYS436
ASP187
ARG186
G
H
LYS A:432
LYS A:190
ARG A:186
ASP A:187
LYS A:432
Interactions
Conventional Hydrogen Bond
Carbon Hydrogen Bond
I
HSA:Tween80
J
ALA191
ASN429
GLN459
LYS190
HIS146
GLU425
ASP108
K
L
ALA A:191
GLN A:459
GLU A:425
ASP A:108
ARG A:186
LYS A:190
ASN A:429
HIS A:146
Interactions
Conventional Hydrogen Bond
Carbon Hydrogen Bond
Alkyl

Supplementary Figure S11. Different views of the most probable complexes of human serum albumin (HAS, PDB ID: 1AO6) and (A-D) GMC, (E-H) PEG400 and (I-L) Tween80. Ball and stick models are GMC, PEG400, or Tween80.

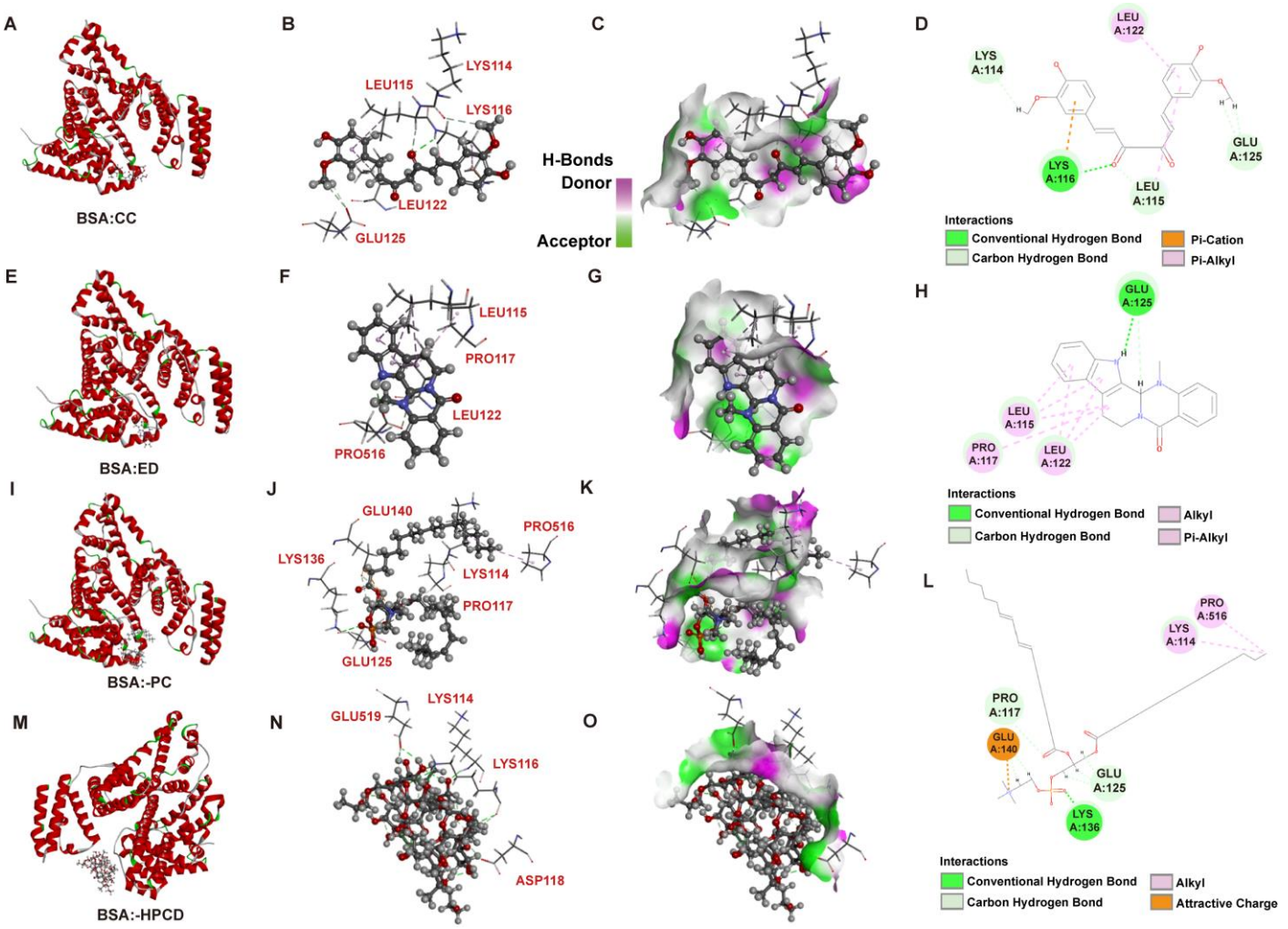
A
BSA:CC
B
LYS114
LEU115
LYS116
LEU122
GLU125
C
H-Bonds
Donor
Acceptor
D
LEU A:122
LYS A:114
GLU A:125
LYS A:116
LEU A:115
Interactions
Conventional Hydrogen Bond
Carbon Hydrogen Bond
Pi-Cation
Pi-Alkyl
E
BSA:ED
F
LEU115
PRO117
LEU122
PRO516
G
H
GLU A:125
LEU A:115
PRO A:117
LEU A:122
Interactions
Conventional Hydrogen Bond
Carbon Hydrogen Bond
Alkyl
Pi-Alkyl
I
BSA:-PC
J
GLU140
PRO516
LYS136
LYS114
PRO117
GLU125
K
L
PRO A:516
LYS A:114
PRO A:117
GLU A:140
GLU A:125
LYS A:136
Interactions
Conventional Hydrogen Bond
Carbon Hydrogen Bond
Alkyl
Attractive Charge
M
BSA:-HPCD
N
GLU519
LYS114
LYS116
ASP118
O

Supplementary Figure S12. Different views of the most probable complexes of bovine serum albumin (BSA, PDB ID: 4F5S) and (A-D) ED, (E-H) CC, (I-L) PC and (M-O) HPCD. Ball and stick models are ED, CC, PC or HPCD.

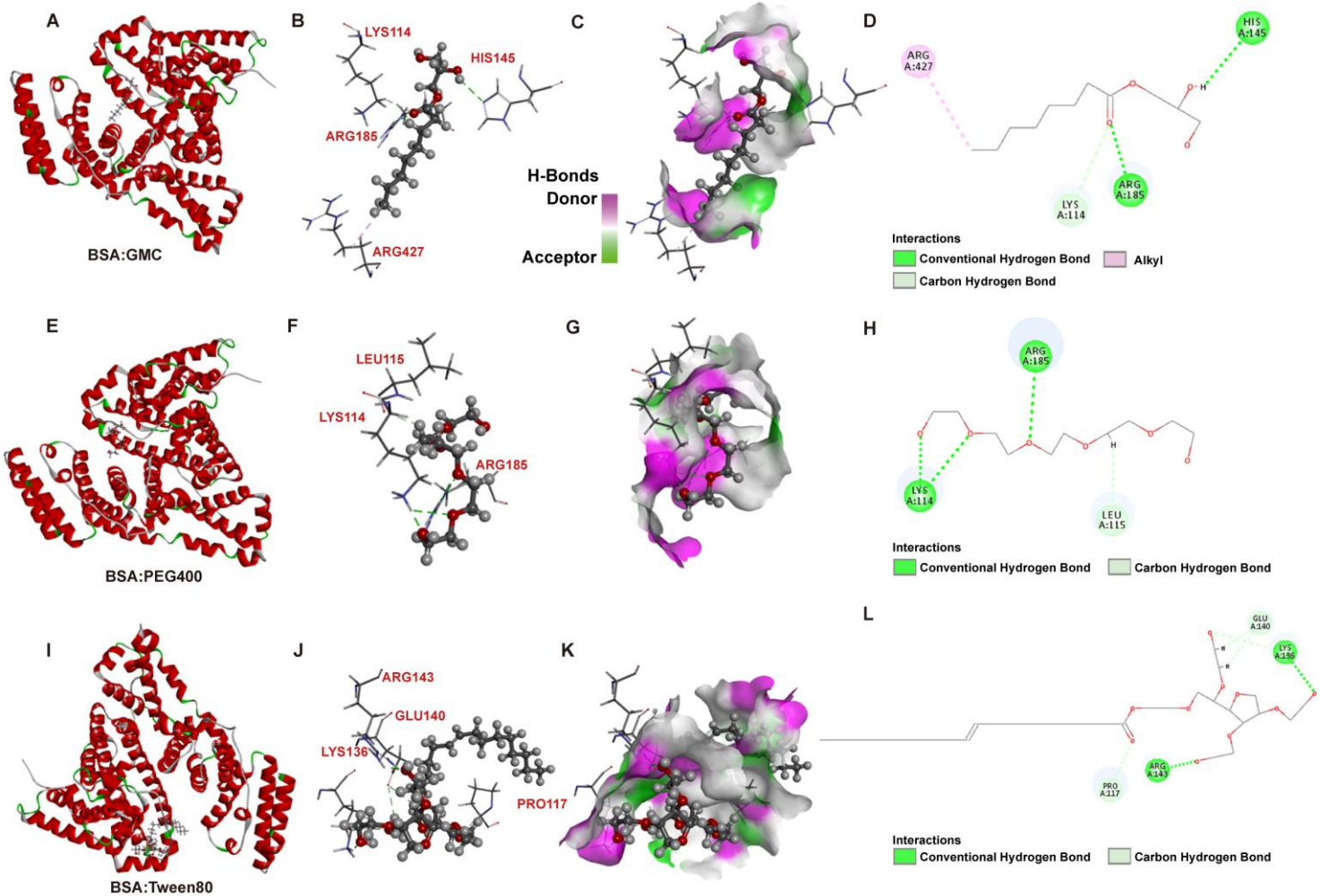
A
BSA:GMC
B
LYS114
HIS145
ARG185
ARG427
C
H-Bonds
Donor
Acceptor
D
HIS A:145
ARG A:427
ARG A:185
LYS A:114
Interactions
Conventional Hydrogen Bond
Alkyl
Carbon Hydrogen Bond
E
BSA:PEG400
F
LEU115
LYS114
ARG185
G
H
ARG A:185
LYS A:114
LEU A:115
Interactions
Conventional Hydrogen Bond
Carbon Hydrogen Bond
I
BSA:Tween80
J
ARG143
GLU140
LYS136
PRO117
K
L
GLU A:140
LYS A:136
ARG A:143
PRO A:117
Interactions
Conventional Hydrogen Bond
Carbon Hydrogen Bond

Supplementary Figure S13. Different views of the most probable complexes of bovine serum albumin (BSA, PDB ID: 4F5S) and (A-D) GMC, (E-H) PEG400 and (I-L) Tween80. Ball and stick models are GMC, PEG400, or Tween80.

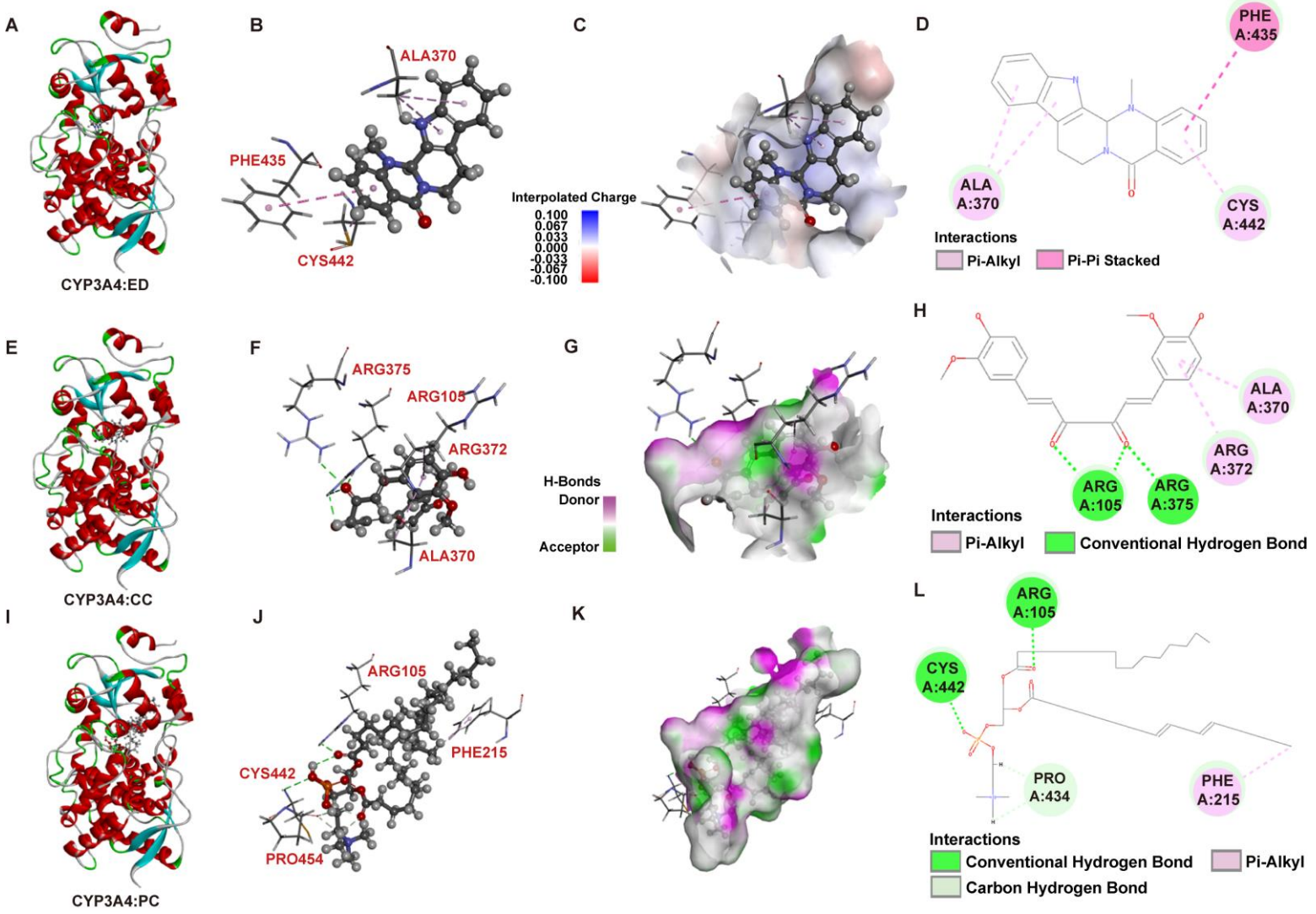
A
CYP3A4:ED
B
ALA370
PHE435
CYS442
C
Interpolated Charge
0.100
0.067
0.033
0.000
-0.033
-0.067
-0.100
D
PHE A:435
ALA A:370
CYS A:442
Interactions
Pi-Alkyl
Pi-Pi Stacked
E
CYP3A4:CC
F
ARG375
ARG105
ARG372
ALA370
G
H-Bonds
Donor
Acceptor
H
ALA A:370
ARG A:372
ARG A:105
ARG A:375
Interactions
Pi-Alkyl
Conventional Hydrogen Bond
I
CYP3A4:PC
J
ARG105
PHE215
CYS442
PRO454
K
L
ARG A:105
CYS A:442
PRO A:434
PHE A:215
Interactions
Conventional Hydrogen Bond
Pi-Alkyl
Carbon Hydrogen Bond

Supplementary Figure S14. Different views of the most probable complexes of cytochromeP450 3A4 (CYP3A4, PDB ID: 1W0E) and (A-D) ED, (E-H) CC and (I-L) PC. Ball and stick models are ED, CC or PC.

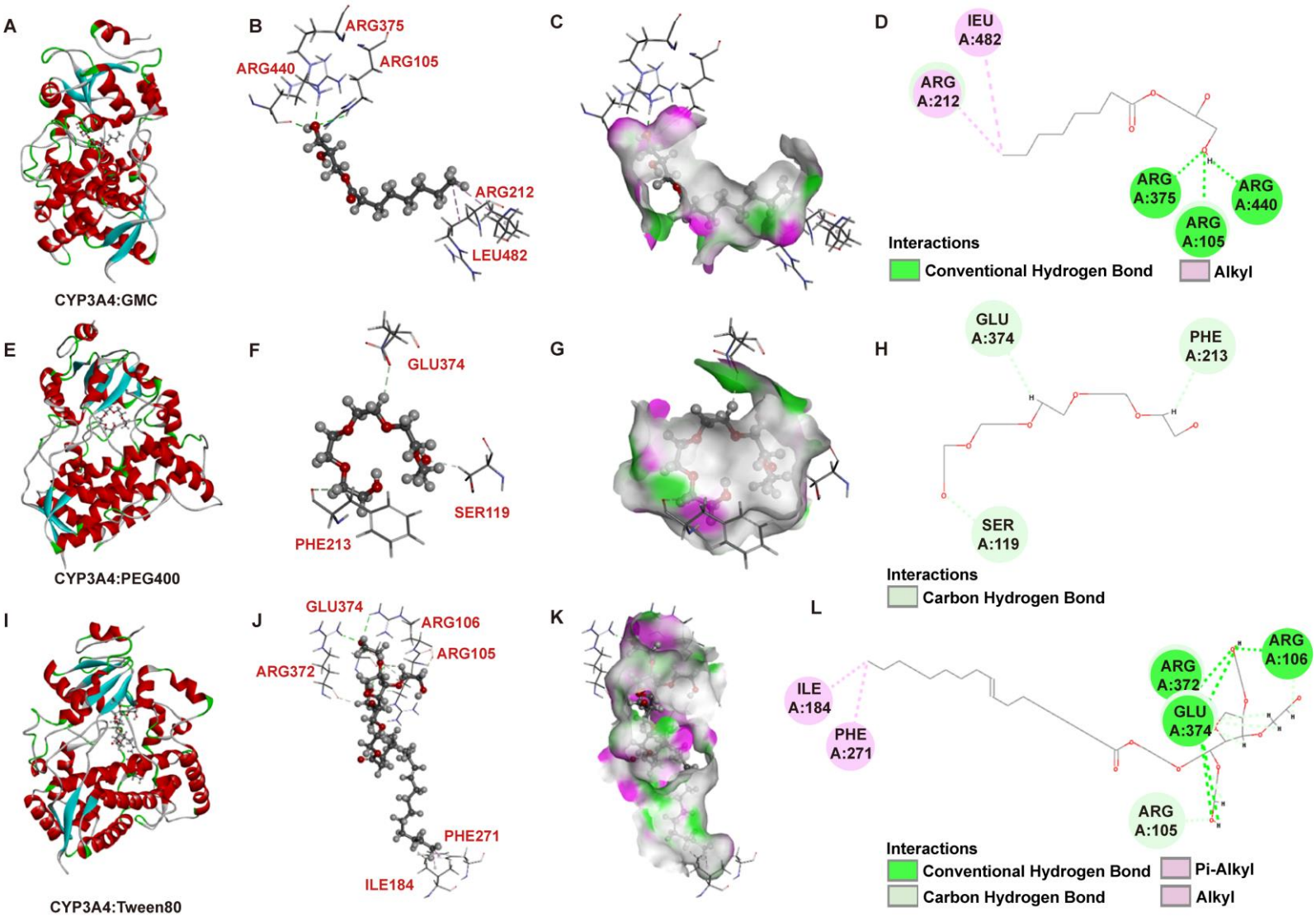
A
CYP3A4:GMC
B
ARG375
ARG105
ARG440
ARG212
LEU482
C
D
IEU
A:482
ARG
A:212
ARG
A:375
ARG
A:440
ARG
A:105
Interactions
Conventional Hydrogen Bond
Alkyl
E
CYP3A4:PEG400
F
GLU374
SER119
PHE213
G
H
GLU
A:374
PHE
A:213
SER
A:119
Interactions
Carbon Hydrogen Bond
I
CYP3A4:Tween80
J
GLU374
ARG106
ARG105
ARG372
PHE271
ILE184
K
L
ARG
A:106
ARG
A:372
GLU
A:374
ILE
A:184
PHE
A:271
ARG
A:105
Interactions
Conventional Hydrogen Bond
Pi-Alkyl
Carbon Hydrogen Bond
Alkyl

Supplementary Figure S15. Different views of the most probable complexes of cytochromeP450 3A4 (CYP3A4, PDB ID: 1W0E) and (A-D) GMC, (E-H) PEG400 and (I-L) Tween80. Ball and stick models are GMC, PEG400, or Tween80.

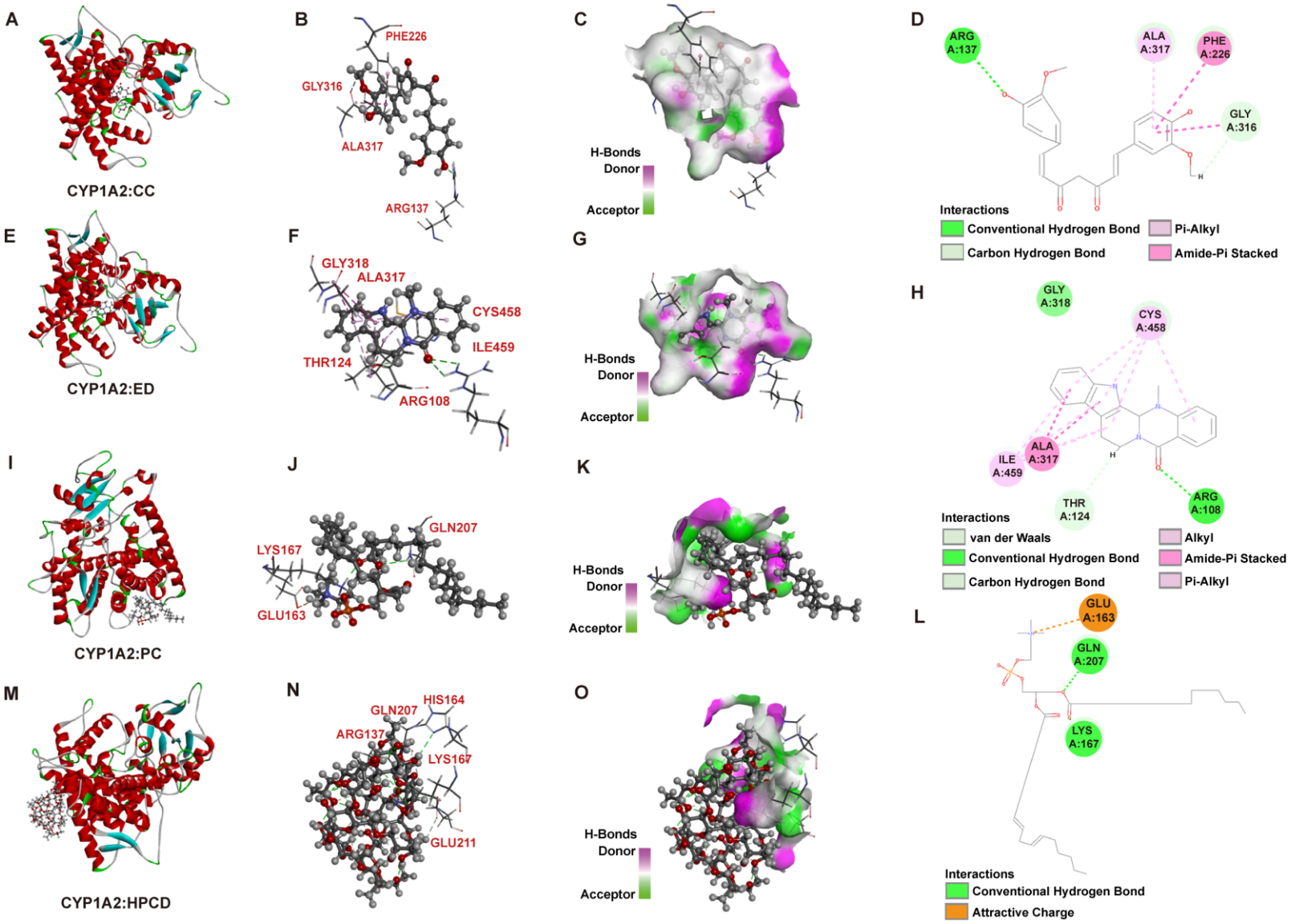
A
CYP1A2:CC
B
PHE226
GLY316
ALA317
ARG137
C
H-Bonds
Donor
Acceptor
D
ARG A:137
ALA A:317
PHE A:226
GLY A:316
Interactions
Conventional Hydrogen Bond
Pi-Alkyl
Carbon Hydrogen Bond
Amide-Pi Stacked
E
CYP1A2:ED
F
GLY318
ALA317
CYS458
ILE459
THR124
ARG108
G
H-Bonds
Donor
Acceptor
H
GLY A:318
CYS A:458
ILE A:459
ALA A:317
THR A:124
ARG A:108
Interactions
van der Waals
Alkyl
Conventional Hydrogen Bond
Amide-Pi Stacked
Carbon Hydrogen Bond
Pi-Alkyl
I
CYP1A2:PC
J
GLN207
LYS167
GLU163
K
H-Bonds
Donor
Acceptor
L
GLU A:163
GLN A:207
LYS A:167
Interactions
Conventional Hydrogen Bond
Attractive Charge
M
CYP1A2:HPCD
N
HIS164
GLN207
ARG137
LYS167
GLU211
O
H-Bonds
Donor
Acceptor

Supplementary Figure S16. Different views of the most probable complexes of cytochromeP450 1A2 (CYP1A2, PDB ID: 2HI4) and (A-D) ED, (E-H) CC, (I-L) PC and (M-O) HPCD. Ball and stick models are ED, CC, PC or HPCD.

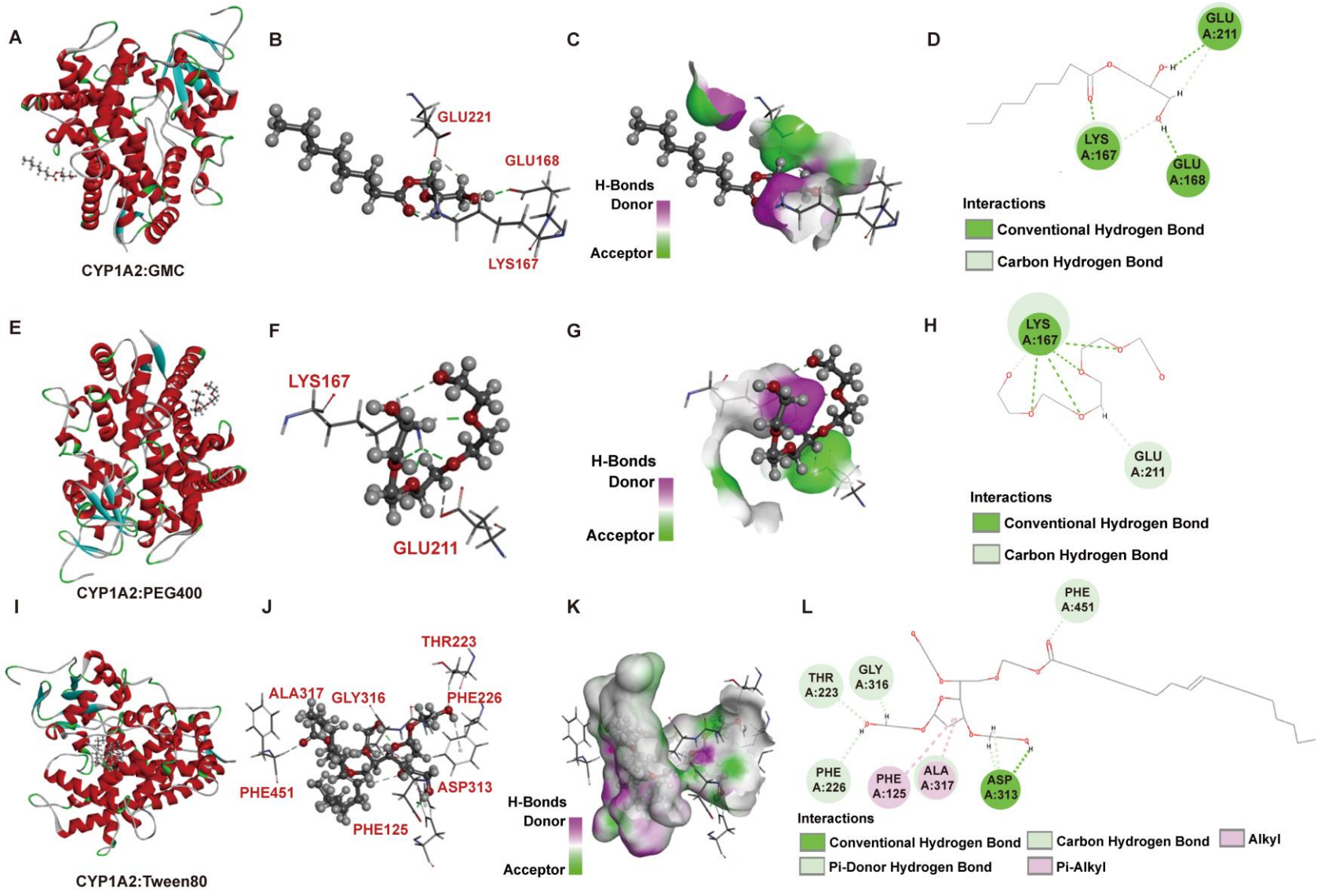
A
B
C
D
GLU221
GLU168
LYS167
H-Bonds
Donor
Acceptor
GLU
A:211
LYS
A:167
GLU
A:168
Interactions
Conventional Hydrogen Bond
Carbon Hydrogen Bond
CYP1A2:GMC
E
F
G
H
LYS167
GLU211
LYS
A:167
GLU
A:211
CYP1A2:PEG400
I
J
K
L
THR223
ALA317
GLY316
PHE226
PHE451
ASP313
PHE125
PHE
A:451
THR
A:223
GLY
A:316
PHE
A:226
PHE
A:125
ALA
A:317
ASP
A:313
Pi-Donor Hydrogen Bond
Pi-Alkyl
Alkyl
CYP1A2:Tween80

Supplementary Figure S17. Different views of the most probable complexes of cytochromeP450 1A2 (CYP1A2, PDB ID: 2HI4) and (A-D) GMC, (E-H) PEG400 and (I-L) Tween80. Ball and stick models are GMC, PEG400, or Tween80.

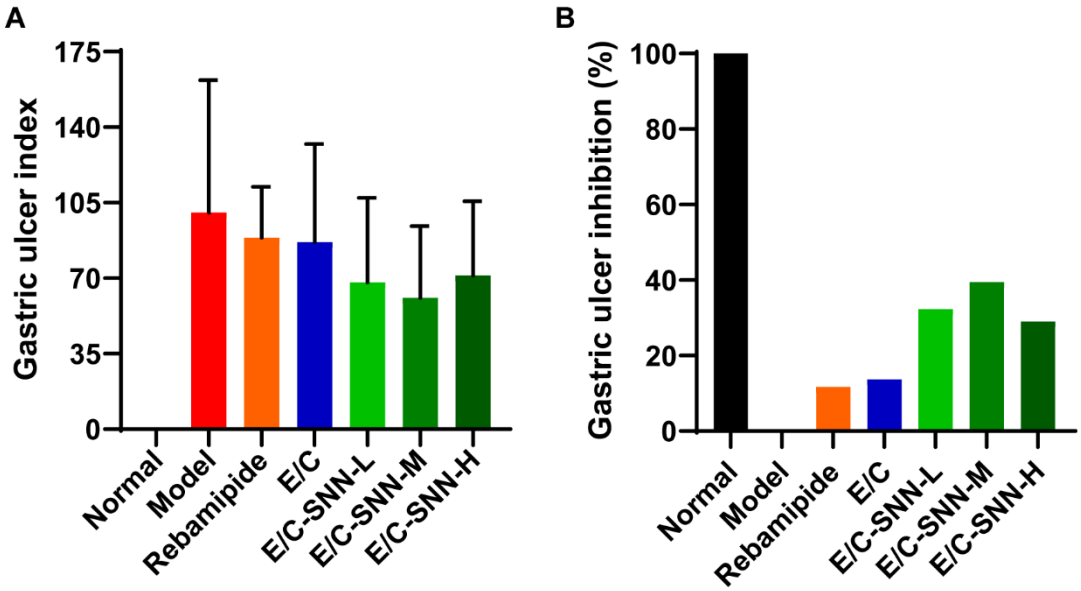

Supplementary Figure S18. Mucosal lesion assessment. (A) Gastric ulcer index and (B) gastric ulcer inhibition rate.

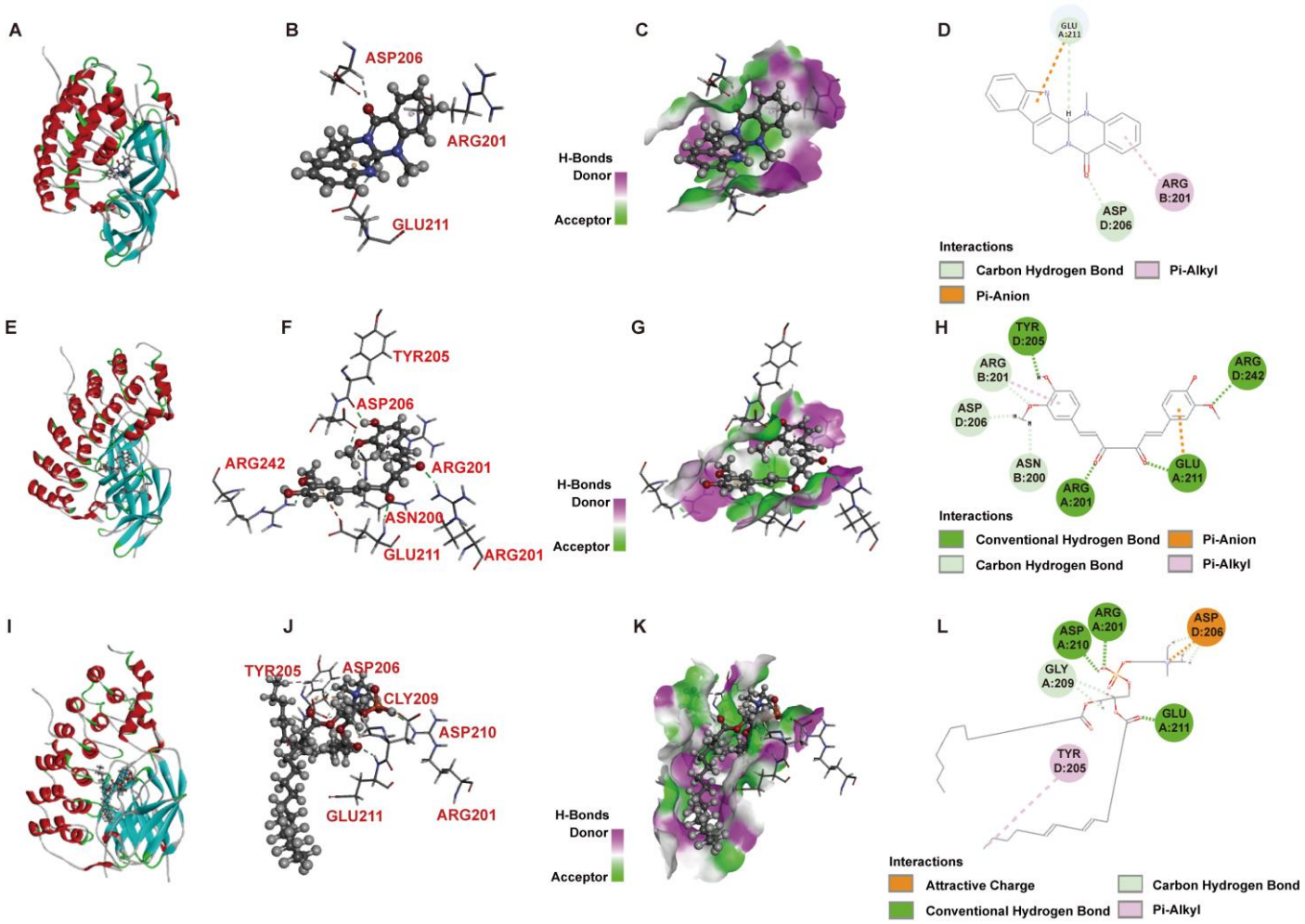

Supplementary Figure S19. Different views of the most probable complexes of IκBβ/NF-κB p65 dimer complex and (A-D) ED and (E-H) CC and (I-L) PC. Ball and stick models are ED, CC or PC.

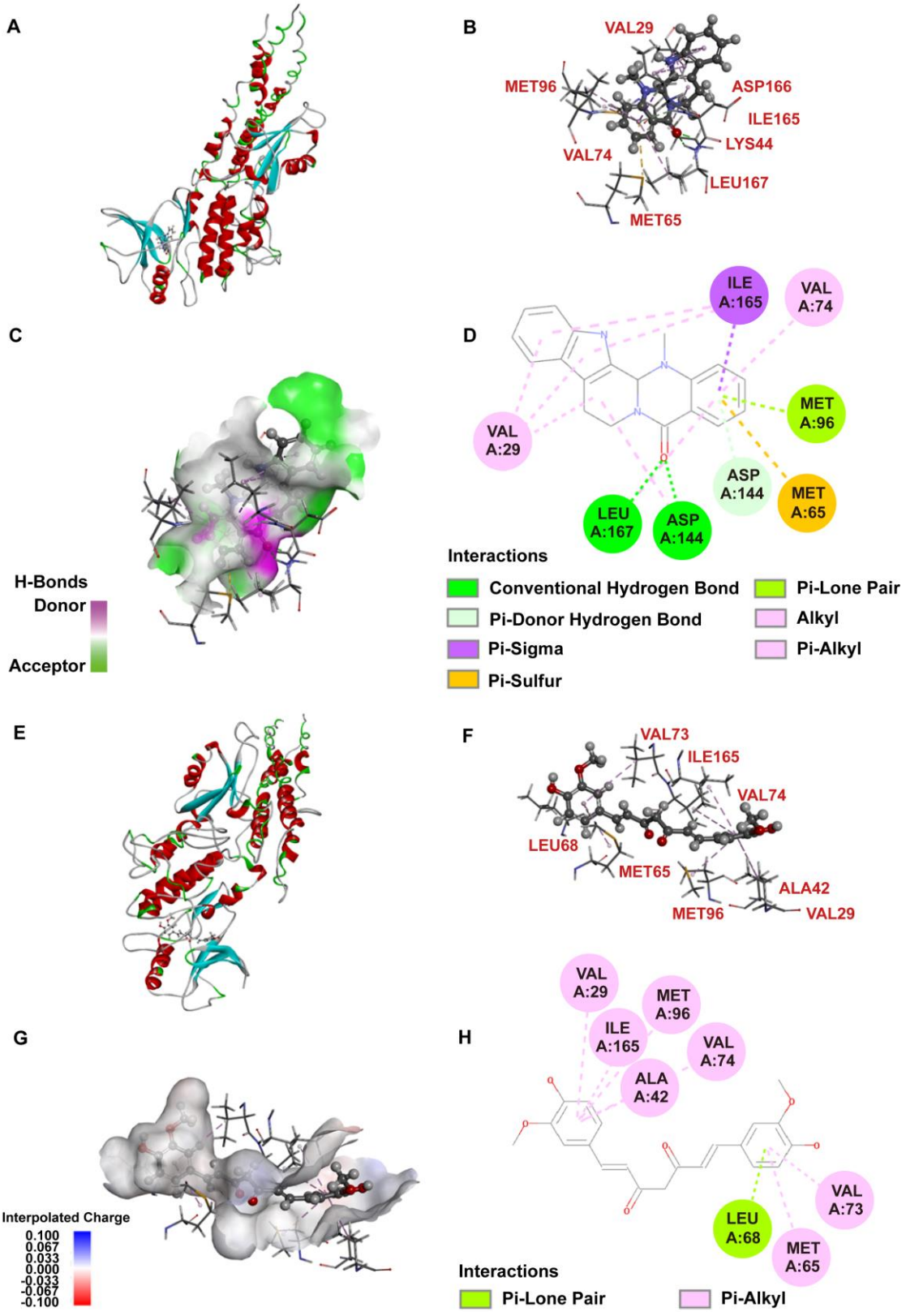

Supplementary Figure S20. Different views of the most probable complexes of IKK and (A-D) ED and (E-H) CC. Ball and stick models are ED or CCM.

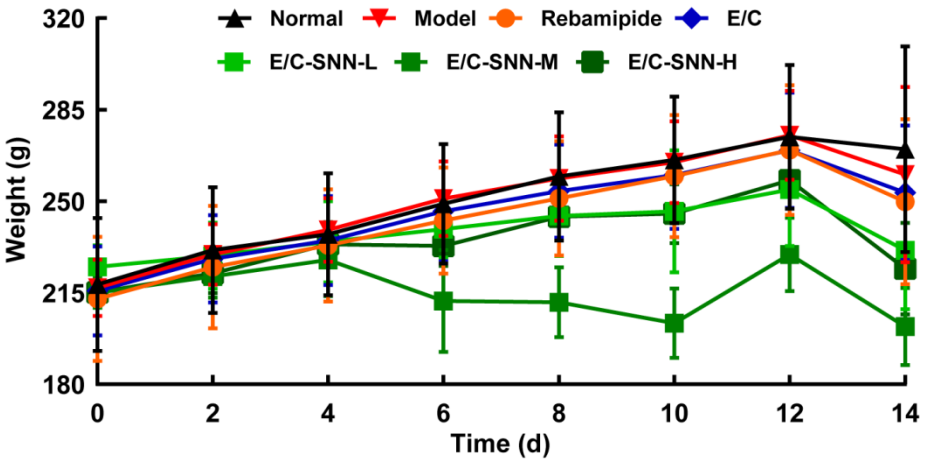

Supplementary Figure S21. Changes of body weight in rats of different groups during experimental period.

Table S1. Gastric lesion score standards

Damage degree	0 point	1 point	2 points	3 points	4 points
Bleeding point	0	1			
Length of bleeding band (mm)	<1 mm	1-5 mm	6-10 mm	10-15 mm	＞15 mm
Width of bleeding zone (mm)	<1 mm	1-2 mm	＞2 mm		

Supplementary Methods and Results

Characteristics of E/C-SNs

The five samples (1. ED, 2. CC, 3. physical mixture of PC and HPCD, 4. physical mixture of ED, CC, PC and HPCD, 5. E/C-SN) were mixed with KBr and analyzed with a Fourier transform infrared (FT-IR) spectrophotometer (Thermo Scientific Instruments, USA), respectively.

The seven samples (1. ED, 2. CC, 3. physical mixture of ED and CC, 4. physical mixture of PC and HPCD, 5. physical mixture of ED, CC, PC and HPCD, 6. Blank E/C-SN, 7. E/C-SN) were heated at the speed of 5 °C/min with a differential scanning calorimetry (DSC) calorimeter (Selb, Germany), respectively.

The results of FT-IR and DSC confirmed the formation of E/C-SN (Fig. S2). In the case of FT-IR analysis, the characteristic peaks of ED were 3222.16 cm^{-1} (-NH), 1631.58 cm^{-1} and 1509.42 cm^{-1} (benzene ring) and 746.54 cm^{-1} and 736.57 cm^{-1} (ortho-substituents on the benzene ring); the characteristic peaks of CC were 3502.65 cm^{-1} (-OH), 1627.98 cm^{-1} and 1508.57 cm^{-1} (benzene ring) and 1283.07 cm^{-1} (-OCH3); the characteristic peaks of PC were 3366.83 cm^{-1} (-OH), 1734.13 cm^{-1} (-C=O), 1240.44 cm^{-1} (-P=O) and 1090.02 cm^{-1} (P-O-C); the characteristic peaks of HPCD were 3393.87 cm^{-1} (-OH). The spectra of the physical mixture of ED, CC, PC and HPCD showed the characteristic peaks of the respective monomers at the same time, which was just a simple addition of the absorption peaks of the respective monomers. The spectrum of E/C-SN was different from the spectra of ED, CC, the mixture of PC and HPCD, as well as the mixture of ED, CC, PC and HPCD. In the spectrum of E/C-SN, the characteristic peaks of ED (746.54 cm^{-1} and 736.57 cm^{-1}) were disappeared and the characteristic peaks of benzene ring of ED (1631.58 cm^{-1} and 1509.42 cm^{-1}) were significantly weakened, so do the peaks of benzene ring of CC (1627.98 cm^{-1} and 1508.57 cm^{-1}). Although the above peaks (1631.58 cm^{-1} and 1509.42 cm^{-1}, 1627.98 cm^{-1} and 1508.57 cm^{-1}) in the spectrum of the mixture of ED, CC, PC and HPCD were weakened to a certain extent, the peaks were weakened more obviously in the spectrum of the E/C-SN. In addition, in the spectrum of E/C-SN, the characteristic peak of ED at 3222.16 cm^{-1} (-NH) and the characteristic peak of CC at 3502.65 cm^{-1} (-OH) were both blunt, mainly showing the characteristic peak of the excipient HPCD at 3393.87 cm^{-1} (-OH).

In the case of calorimetry determination, ED exhibited an endothermic peak at 287.5 ℃, and CC exhibited endothermic peaks at 30.3 ℃ and 174.8 ℃

respectively. The physical mixture of ED and CC exhibited endothermic peaks of the respective monomers at the same time. The physical mixture of PC and HPCD exhibited no obvious endothermic peak below 50℃, but a large depression, which might be the melting process of PC. An endothermic peak appeared at 52.9℃, which was the melting peak of HPCD, and the peak shape was small. In the spectrum of the physical mixture of ED, CC, PC and HPCD, there exhibited no obvious endothermic peak below 50°C, and there was a wide peak at 76.6°C where CC and HPCD formed a cohesive peak. The endothermic peak of CC at 174.8 ℃ was disappeared, and there was a wide peak at 266.6 ℃, where ED and CC formed a cohesive peak. In the DSC spectrum of E/C-SN, new endothermic peaks appeared at 20.4 ℃, 63.4 ℃, and 267.6 ℃, and the endothermic peaks of ED and CC disappeared, and there were obvious differences between the spectrum of the physical mixture (ED, CC, PC, HPCD). Above all, the results suggested that E/C-SN were successfully prepared.

Mucosal lesion assessment

The lesion size of stomach was measured with a Vernier caliper and a magnifying glass, and calculated the gastric ulcer index (GUI) according to the file approved by China Food and Drug Administration[1, 2] and the documented revised method [3]. The gastric lesion was scored according to the Table S1. The GUI value was calculated according to formula 1.

$$GUI = \text{bleeding point score} + \text{length score} + (\text{width score} \times 2) \quad (1)$$

The gastric ulcer inhibition rate (%) of each group was according to formula 2.

$$\text{Inhibition} = (GUI_{model} - GUI_{test}) / GUI_{model} \times 100\% \quad (2)$$

The gastric ulcer indexes decreased in the turn of the model group (100.45±61.28), rebamipide group (88.68±23.71), E/C group (86.72±45.41,), E/C-SNN-L group (68.00±39.20), E/C-SNN-M group (60.83±39.44), and E/C-SNN-H group (71.30±34.37), respectively (Fig. S18A). The inhibition rates increased in the turn of the model group (100.45±61.28, 0%), rebamipide group (11.72%), E/C group (13.67%), E/C-SNN-L group (32.30%), E/C-SNN-M group (39.44%), and E/C-SNN-H group (29.02%), respectively (Fig. S18B).

Reference

1. M. Beiranvand, S. Bahramikia and O. Dezfoulian, *Inflammopharmacology*, 2021, **29**(5), 1503-1518. [PubMed: 34435283].
2. P. H. Guth, D. Aures and G. Paulsen, *Gastroenterology*, 1979, **76**(1), 88-93. [PubMed: 361495].
3. S. Ren, Y. Wei, R. Wang, S. Wei, J. Wen, T. Yang, X. Chen, S. Wu, M. Jing, H. Li, M. Wang and Y. Zhao, *Front Pharmacol*, 2020, **11**, 600295. [PubMed: 33324227].